

See discussions, stats, and author profiles for this publication at: <https://www.researchgate.net/publication/244136942>

$(2 + n)$ REMPI of acetylene: Gerade Rydberg states and photorupture channels

ARTICLE *in* CHEMICAL PHYSICS LETTERS · JUNE 2008

Impact Factor: 1.9 · DOI: 10.1016/j.cplett.2008.04.104

CITATIONS

5

READS

14

3 AUTHORS, INCLUDING:



[Huasheng Wang](#)

University of Iceland

34 PUBLICATIONS 294 CITATIONS

[SEE PROFILE](#)



[Agust Kvaran](#)

University of Iceland

87 PUBLICATIONS 1,111 CITATIONS

[SEE PROFILE](#)



(2 + n) REMPI of acetylene: Gerade Rydberg states and photorupture channels

Kristján Matthíasson, Huasheng Wang, Ágúst Kvaran *

Science Institute, University of Iceland, Dunhagi 3, 107 Reykjavík, Iceland

ARTICLE INFO

Article history:

Received 27 February 2008

In final form 23 April 2008

Available online 29 April 2008

ABSTRACT

Mass analysis studies were performed of ions detected after (2 + n) REMPI of acetylene for resonance excitations to various gerade Rydberg states as a function of laser power. These data, along with STQN/DFT calculations for dissociation of acetylene to $C_2 + H_2$, allowed an estimate of a threshold for photodissociation via gerade Rydberg states near $75\,000\text{--}77\,000\text{ cm}^{-1}$. Mechanisms are proposed regarding (2 + 3) REMPI of acetylene to form C_2^+ as well as C^+ and H^+ . Simulation analysis of partly-resolved rotational structured spectra recorded for different jet cooling allowed determinations of precise spectroscopic parameters and lifetime estimates for the Rydberg state, $4p\ ^1\Delta_g 0^0$.

© 2008 Elsevier B.V. All rights reserved.

1. Introduction

UV spectroscopy, photochemistry and photophysics of acetylene (C_2H_2) have been widely studied over the recent years. This is partly due to its importance in interstellar space and cometary atmospheres, where it is one of the most abundant species observed. There it has been considered to be a reservoir molecule for the production of carbon-containing radicals which, in turn, are involved in formation of larger organic compounds [1–3]. Furthermore, being the simplest unsaturated hydrocarbon, acetylene is a fundamental unit in various organic photochemistry processes and synthesis work.

Photodissociation of C_2H_2 has been the subject of numerous experimental investigations, among which are studies by single- [1,2,4–8], two- [9,10] and three- [2,4] photon resonance excitations. Photodissociation in acetylene is almost exclusively found to occur via excitations to high-lying Rydberg states $C_2H_2^*$. Due to the strict $u \leftrightarrow g$ selection for excitation per photon interaction only ungerade Rydberg states are accessed by one- and three- (odd number) photon excitations from the $1^1\Sigma_g^+$ electronic ground state, whereas gerade Rydberg states are accessible by two-photon (even number) excitation. In view of this, and the additional restriction on possible intersystem crossings based on the selection rules $u \leftrightarrow u$ and $g \leftrightarrow g$, it is not surprising that the mechanism and outcome of photodissociation differ in accord with on odd- or even-number photon excitations. Fragmentation of C_2H_2 into C_2H and H is found to be dominant following single- and three-photon excitations [1,6,10]. Thus single-photon excitations of the Rydberg states below the first ionisation potential reveal only the C_2H product by emission spectra [6]. Two distinct dissociation channels, fol-

lowing single-photon excitations, have been observed [7,8], showing major differences with respect to internal energies and angular distributions of the fragments C_2H and H . In both channels the observed decay dynamics are found to depend strongly on the excited state of the parent molecule, $C_2H_2^*$. In the case of a predissociation of the C_2H_2 ($H^1\Pi_u$) Rydberg state, it has been proposed that it occurs via the bent valence state A^1A_u [7]. From less extensive two-photon excitation studies, on the other hand, fragmentations both into $C_2 + H_2$ and into $C_2H + H$, are found to occur [9,11]. Thus C_2 molecules in the $X^1\Sigma_g^+$, $a^3\Pi_u$, $A^1\Pi_u$ and $d^3\Pi_g$ states, H atoms and H_2 molecules have been identified by time-resolved photofragment and emission detection studies [9,11]. Both sequential bond-rupture mechanisms and concerted two-bond fission processes have been proposed to explain the C_2 and H_2 fragment formations [11]. Furthermore, long-lived bent isomers of C_2H_2 , as well as C_2H intermediates, have been revealed experimentally. Tsuji et al. concluded from detailed REMPI analysis [9] that ion fragment formations are predominantly due to ionisation of neutral molecular fragments after predissociation. Because of the characteristic predissociation channels, the ungerade and gerade Rydberg states of acetylene are found to be short-lived, with lifetimes ranging from 50 fs to more than 10 ps [4,9]. Despite extensive experimental and theoretical studies on the photochemistry of acetylene, many unsettled questions remain regarding the mechanism of its photodissociation [9].

Rotational spectra due to electronic transitions recorded by resonance-enhanced-multiphoton-ionisation (REMPI) [4,9,12,13], absorption [4,14] or as fluorescence excitation spectra [9] suffer from line broadenings depending on the Rydberg state lifetimes. Hence either nonresolved or partly-resolved rotational structures are observed, limiting detailed studies of the excited states involved. A number of rotationally-structured spectra due to transitions to ungerade Rydberg states have been recorded and analysed to derive rotational parameters [13,14] and/or lifetime values [4]

* Corresponding author. Fax: +354 552 8911.

E-mail address: agust@hi.is (Á. Kvaran).

URL: <http://www.hi.is/~agust/> (Á. Kvaran).

Table 1Band origins (ν^0) rotational parameters (B and D) and lifetimes (τ) for C_2H_2 electronic states

Species	ν^0/cm^{-1}	u-States;	g-States;	ν	B/cm^{-1}	$D/10^{-6} \times \text{cm}^{-1}$	τ (lifetimes)
C_2H_2 ground state $\text{C}_2\text{H}_2^{**}$ Rydberg states	0		$X^1\Sigma_g^+$		1.17660 ^{a,b,c,d}	1.61 ^{a,b,c}	
	79933	$3d\delta, ^1\Phi_u^i$		$\nu = 0^b$	1.105 ^b	(1.5) ^{b,f}	>10 ps ^m
	80111 ^h	$G\ 4s\sigma, ^1\Pi_u^h$		$\nu = 0^h$	1.1023(1) ^{i,j}	1.5(2) ^{i,j}	>10 ps ^{h,k}
	80154 ⁱ	$G\ 4s\sigma, ^1\Pi_u^i$		$\nu_4 = 1^i$	1.100(1) ^{i,j}	(1.5) ^{f,i}	
	81695 ^h	$F^3d\delta, ^1\Phi_u^h$		$\nu_2 = 1^h$	1.104(1) ^{i,j}	(1.5) ^{f,i}	~1 ps ^{b,h}
	82562 ^d		$4p, ^1\Delta_g^d$	$\nu = 0$	(1.115) ^{d,f}	–	(>2.1 ps) ^d
	82556 ± 2^l		$4p, ^1\Delta_g$	$\nu = 0$	1.110 ± 0.001^l	0.99 ± 0.02^l	>2.6 ps ^l
	85229 ^h	$I\ 5s\sigma, ^1\Pi_u^h$		$\nu = 0^h$	1.09955(54) ⁱ	2.1(7) ^{i,j}	~3 ps ^{h,m}
	85425 ^h	$J\ 4d\delta, ^1\Pi_u^h$		$\nu = 0^h$	1.107(2) ^{i,j}	5.5(33) ^{i,j}	~2 ps ^{h,m}
	87054 ^h	$I\ 5s\sigma, ^1\Pi_u^h$		$\nu_2 = 1^h$	1.0933(4) ^{i,j}	0.9(5) ^{i,j}	~2 ps ^{h,i}
	87884 ⁱ				1.076(3) ^{i,j}	(0) ^{i,3}	
	88852 ⁱ	$I\ 5s\sigma, ^1\Pi_u^i$		$\nu_2 = 2^i$	1.084(1) ^{i,j}	–10(2) ⁱ	
	89266 ⁱ				1.097(5) ^{i,j}	26(20) ^{i,j}	
	89751 ⁱ	$M\ 8s\sigma, ^1\Pi_u^i$		$\nu = 0^i$	1.0932(7) ^{i,j}	(0) ^{i,f}	
	90630 ⁱ	$N10s\sigma, ^1\Pi_u^i$		$\nu = 0^i$	1.1006(6) ^{i,j}	–6.0(5) ^{i,j}	
	91956 ⁿ	$X^2\Pi_u$		$\nu = 0$	1.104 ^{d,o}		
C_2H_2^+ ground ion state							

^a Ref. [22].^b Ref. [13].^c Ref. [32].^d Ref. [9].^f Imposed value.^h Ref. [4].ⁱ Ref. [14].^j Errors (in parentheses) are expressed in units of the last digits.^k Ref. [1].^l This work.^m Ref. [2].ⁿ Ionization potential [3].^o Ref. [33].

for the excited states (see Table 1). Analyses of one-photon absorption spectra allowed determinations of fairly precise rotational parameters [14] whereas more tentative values have been obtained from three-photon resonance excitation experiments [13]. Lifetimes of very short-lived states have been determined by means of photofragment action spectroscopy [7]. Only spectra due to transitions to one gerade Rydberg state with partially resolved rotational structures, have been reported for C_2H_2 . Tentative analyses of these spectra have been performed with an emphasis on assigning the corresponding Rydberg states. Lifetimes of gerade Rydberg states have been estimated from spectral bandwidths [9]. Rotational parameters have been derived for states with lifetimes larger than about 1 ps only.

In this Letter we emphasise two-photon resonance excitations of acetylene to gerade Rydberg states followed by ionisation, i.e. $(2+n)$ REMPI. We present ion mass-analysis as a function of laser excitation frequencies and laser power, combined with DFT/STQN [15,16] calculations on $\text{C}_2\text{H}_2 \rightarrow \text{C}_2 + \text{H}_2$ surfaces, which, together with energetic interpretations, allows determination of important thresholds for fragmentation processes. Furthermore we report a thorough analysis of partly rotationally-resolved structured spectra due to the $4p\ ^1\Delta_g \leftarrow X^1\Sigma_g^+$ transition recorded for different jet cooling, which allows a derivation of precise rotational and vibrational parameters for the $4p\ ^1\Delta_g$ Rydberg state.

2. Experimental

Resonance-enhanced-multiphoton-ionisation (REMPI) of jet-cooled C_2H_2 gas was performed in an ionisation chamber. Ions were directed into a time-of-flight tube by electric lenses and detected by MCP plates to record ion yield as a function of flight time, hence mass, and/or as a function of laser radiation wavenumber. The apparatus has been described elsewhere [17–19].

Tunable excitation radiation in the wavelength region 227–278 nm was generated by an Excimer laser-pumped dye laser sys-

tem, using a Lambda Physik COMPex 205 Excimer laser, a Lumonics Hyperdye 300 laser and frequency doubling with BBO crystals. The repetition rate was typically 5 Hz for about 10 ns laser pulses. The bandwidth of the dye laser beam was about 0.05 cm^{-1} . Laser pulse energies used were in the range 0.05–0.32 mJ/pulse. The radiation was focused with a 200 mm focal-length quartz lens into an ionisation chamber between a repeller and an extractor separated by 19 mm. Gas samples, either pure C_2H_2 (AAS Acetylene 2.6 from Linde gas) or mixtures of C_2H_2 and argon (typically in ratios ranging from 1:1 to 1:9 = $\text{C}_2\text{H}_2:\text{Ar}$) were pumped through a 500 μm pulsed nozzle from a typical total backing pressure of about 0.6–1.8 bar into the ionisation chamber, which was maintained at lower than about 10^{-5} mbar pressure during experiments. The distance from the nozzle to the centre between the repeller and the extractor was about 6 cm. The nozzle was held open for about 200 μs and the LASER beam was typically fired about 450 μs after opening the nozzle. Ions were extracted into a 70 cm-long time-of-flight tube and focused with an electric lens onto a MCP plate detector. Voltage outputs as a function of flight time were fed into a LeCroy 9310A 400 MHz storage oscilloscope. Average voltage outputs for a fixed number of laser pulses were evaluated and recorded on a computer to produce mass spectra. Either mass peak heights or integrals were measured and averaged for a fixed number of laser pulses as a function of laser radiation wavenumbers to obtain REMPI-TOF spectra. Typically spectral points were obtained by averaging over 200 pulses.

Wavelength calibration was achieved by recording iodine atomic lines [20] or by measurements of the strongest hydrogen chloride rotational lines and comparison with those reported by Green et al. [21]. The accuracy of the calibration was found to be about $\pm 1.0\text{ cm}^{-1}$ on a two-photon wavenumber scale. Care was taken to correct for possible drifts in signal intensity during long scans. Spectra intensities were corrected for possible intensity drift during the scan. Furthermore, the effect of varying laser power was corrected for by dividing the measured intensity by the power squared.

3. Results and analysis

3.1. Mass spectra: analysis and interpretations

Fig. 1, left, shows some REMPI spectra for two-photon resonance excitations obtained by recording maximum ion signals as a function of excitation wavenumbers. The main spectral features, all due to resonance transitions to gerade Rydberg states, have been identified before [9,12], and are assigned accordingly. No Rydberg states could be detected for higher energies, whereas weak $(1+n)$ REMPI due to the transition $A^1A_u \leftarrow X^1\Sigma_g^+$ was observed in the region $84\,000\text{--}88\,000\text{ cm}^{-1}$ on the two-photon wavenumber scale, corresponding to the $42\,000\text{--}44\,000\text{ cm}^{-1}$ region on the one-photon wavenumber scale [22], here reported for the first time. Ion mass spectra for 'intermediate' (see explanation below) strength laser power is shown in Fig. 1, right, for the main spectral features. These were obtained by subtracting mass spectra, for background signals close by, from those recorded for the Rydberg spectra in order to obtain contributions due to the resonance excitations.

The parent molecular ion, $C_2H_2^+$, was found to be the dominant ion species formed for the lowest energy 3p-Rydberg resonances (i) $72\,744\text{--}74\,554\text{ cm}^{-1}$ showing an increase with laser power, while negligible or no other fragment ions were detected. This is analogous to what others have found [12]. The resonance signals at (ii) $75\,760\text{ cm}^{-1}$ and $76\,085\text{ cm}^{-1}$ (3p Rydberg states) show a number of ion-fragment signals such as H^+ , C^+ , CH^+ , C_2^+ , C_2H^+ , as well as the parent molecular ion $C_2H_2^+$. The ratios of ion signals for H^+ , C^+ , and C_2^+ to that of the parent ion were found to increase proportionally with laser power for all the fragment ions. The Rydberg resonance signals for the 4p states at (iii) $82\,561\text{ cm}^{-1}$ and $83\,006\text{ cm}^{-1}$ were far weaker than those for the 3p states, showing the fragment ions dominating the parent ion. Only a weak $C_2H_2^+$ ion signal is observed at $82\,561\text{ cm}^{-1}$, and the fragment ion signals all increased proportionally relative to that of the parent ion. No significant $C_2H_2^+$ could be observed at $83\,006\text{ cm}^{-1}$. The mass spectra shown in Fig. 1, right, were chosen for 'intermediate' laser powers suitable to demonstrate the main features observed and trends mentioned. These observations will now be interpreted and discussed with reference to the schematic energy diagrams in Fig. 2 and relevant observations made by others.

All the Rydberg states in question are known to be predissociated. Both fragmentations into $C_2 + H_2$ and into $C_2H + H$ have been postulated [9,11]. This has either been deduced from detections of fragment species [9,11] or based on spectral bandwidth measurements, hence lifetime estimations [9]. Thus C_2 in the excited $d^3\Pi_g$ state has been identified from detection of the fluorescence due to the transition $d^3\Pi_g \rightarrow a^3\Pi_u$ (Swan band) in all cases. The formation of $C_2 d^3\Pi_g$ has been interpreted as being due to predissociation of the gerade Rydberg states to C_2H , followed by a further photodissociation of C_2H [9,11]. According to Tsuji et al. [9] there is reason to believe that the fragment ions detected in REMPI, under comparable conditions to our cases (see above), are generally formed from ionisation of neutral fragments rather than from photofragmentation of the parent ion. In the case of excitation to the $3p^1\Sigma_g^0$ Rydberg state ($74\,279\text{ cm}^{-1}$ band), Hsu et al. propose long-lived intermediates after predissociation [11]. Thus, for example, $C_2 X^1\Sigma_g^+$ and $C_2 d^3\Pi_g$ molecules are believed to be formed primarily by a sequential bond-rupture mechanism via excitation of long-lived C_2H fragments, whereas some C_2 in $a^3\Pi_u$ is formed by a concerted two-bond fission process via excitation of a long-lived *cis* isomer (see Fig. 2a). Insignificant fragment ion formation observed for the (i) $72\,744\text{--}74\,554\text{ cm}^{-1}$ region could be due to slow fragment formation processes on the timescale of the laser detection (about 10 ns laser pulses), causing only direct ionisation of the Rydberg excited molecules to be observed. The sudden alteration from dominant parent ion formation to ion fragments, as well as the parent ion-formation, as excitation increased to (ii) $75\,760\text{ cm}^{-1}$ and $76\,085\text{ cm}^{-1}$, could in principle be due to a sudden alteration in ionisation cross sections. Based on the energetics for C_2^+ formation from ionisation of C_2 (or excited states C_2^*), however, three additional photons (five photons in total; see Fig. 2b) are needed in all cases; hence no sudden alteration in ionisation is to be expected. Therefore this observation is probably due to the opening up of new and/or faster dissociative channel(s) between $74\,554\text{ cm}^{-1}$ and $75\,760\text{ cm}^{-1}$. Dominant fragment ion formations via excitations to the high-lying Rydberg states (iii) $82\,561\text{ cm}^{-1}$ and $83\,006\text{ cm}^{-1}$ and comparable power dependence of ion signals suggests that the dissociative channel(s) is of still greater importance at higher energies. Slight parent ion formation in the case of $82\,561\text{ cm}^{-1}$ excitation is due to the relatively long lifetime of the relevant Rydberg state ($4p^1\Delta_g 0^0$; $\tau > 2.1\text{ ps}$).

In an attempt to search for a threshold energy for $C_2 + H_2$ fragment formation we performed quantum-chemical calculations based on DFT, using a QST- (quadratic synchronous transit [23]) based method and tracked energy paths starting from various singlet and triplet states of C_2H_2 , via an intermediate *cis*-conformer, to the ground state molecular fragments. Thus we looked for transition states in terms of energy and molecular shape. The calculations were performed using the software package GAUSSIAN 98 [24] and the STQN method [15,16] for B3LYP level of calculations and various basis sets (3-21G, 6-31G, 6-31G*, 6-31G**). The lowest energy transition states were obtained for the lowest energy singlet and triplet states of C_2H_2 , but with some variation from one calculation level to another. Comparable energies, for the transition states, were obtained for singlet and triplet states. The lowest transition state energies obtained were about $75\,000\text{ cm}^{-1}$ as seen in Fig. 3 for the 6-31G* basis set. The structure for the singlet transition state is shown in the figure. This result and the above-mentioned experimental data lead us to believe that a faster dissociation process, leading to formations of C_2 and H_2 , occurs in region (ii) ($75\,760\text{ cm}^{-1}$ and $76\,085\text{ cm}^{-1}$) compared to that in region (i) ($72\,744\text{--}74\,554\text{ cm}^{-1}$), involving atom migration to a *cis* configuration and crossing over a transition state ($E = 76\,000 \pm 1000\text{ cm}^{-1}$) on the lowest energy singlet surface for the *cis* conformer (Fig. 3). The C_2^+ observed in REMPI for excitations larger in energy than $75\,000\text{ cm}^{-1}$, will hence be formed after that, by three-photon

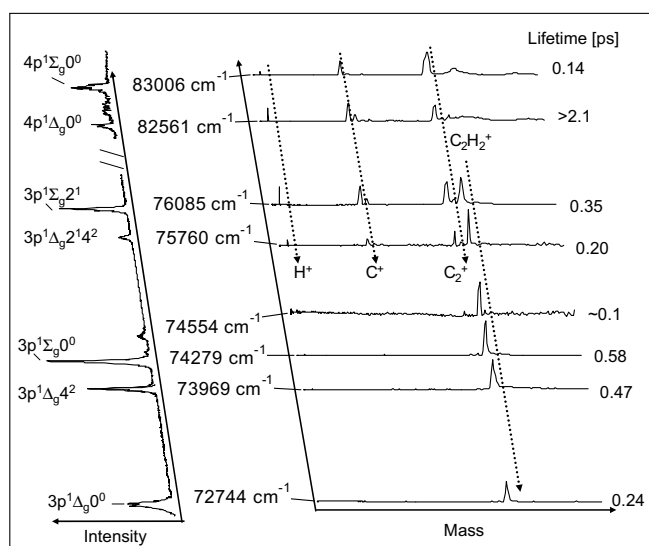


Fig. 1. REMPI spectra and corresponding mass spectra for acetylene; Rydberg state assignments and lifetimes as well as REMPI spectra wavenumber values are indicated.

to $H(n=1) + C_2H$, for excitations into the lowest Rydberg states, whereas three photons are needed to ionise $H(n=1)$ for Rydberg states higher in energies than $75\,000\text{ cm}^{-1}$ (see Fig. 2b).

3.2. REMPI spectra for $4p^1\Delta_g 0^0 \leftarrow X^1\Sigma_g^+$ vs. rotational temperature; simulation analysis

Fig. 4a and b (top) show REMPI spectra due to the resonance transition $4p^1\Delta_g 0^0 \leftarrow X^1\Sigma_g^+$ for different argon:acetylene ratios and/or backing pressures, hence different jet cooling conditions. We performed simulation analysis of a number of such spectra, based on least square analysis of intensities using spectroscopic parameters, bandwidth as well as rotational temperatures as variables, and searched for an unified solution in terms of the parameters and the bandwidth. This method allowed derivations of precise parameter values despite only partly resolved rotational structures.

A simulation analysis method analogous to that used before [26–29] for analysis of two-photon absorption in diatomic molecules, based on derivations of line-strengths for linear molecules [30], was used. Thus rotational line positions were derived from the expression

$$\tilde{\nu}_{J',v' \leftarrow J'',v''} = \tilde{\nu}_{v' \leftarrow v''}^0 + \Delta E_{J,J''}$$

where $(\tilde{\nu}_{v' \leftarrow v''}^0)$ is the band origin of the vibrational band and $\Delta E_{J,J''}$ is the difference in rotational energies in the ground and excited states, depending on the relevant rotational parameters [29].

Relative line intensities (I_{rel}) of spectra at thermal equilibrium were evaluated from

$$I_{\text{rel}} = C g_{J''} (\mu_+ \mu'_+)^2 s(J, \Delta J) \exp(-E(J'')hc/k_B T)$$

where $g_{J''}$ is the degeneracy of level J'' . μ_+ and μ'_+ are the one-photon perpendicular transition moments for transitions via a virtual state in the two-photon excitation [27], treated here as constants. $s(J, \Delta J)$ are relevant Hönl-London factors, which depend on the quantum numbers J' and J'' [30]. $E(J'')$ is the rotational energy in the ground state (in cm^{-1}). h , c , k_B and T have the usual meanings and C is an arbitrary constant. Individual rotational lines were displayed as Gaussian-shaped functions of wavenumbers ($I(\tilde{\nu})$) and bandwidth (bw/cm^{-1}) as [31]

$$I(\tilde{\nu}) = \frac{I_{\text{rel}}}{bw} \exp\left(-\frac{4\ln(2)}{bw^2}(\tilde{\nu} - \tilde{\nu}^0 - \Delta E_{J,J''})^2\right)$$

Finally the lifetime was derived from the relation

$$Bw(\text{cm}^{-1}) = fwhm(\text{cm}^{-1}) = 5.3/\tau(\text{ps})$$

Spectra recorded for limited cooling could be simulated by assuming a thermal distribution (i.e. Boltzmann distribution) as seen in Fig. 4a, whereas a better fit was obtained for ‘colder’ spectra by assuming two temperature components (see Fig. 4b). This latter effect we attribute to a nonthermal/nonequilibrium rotational energy distribution in the beam showing as a population tail to higher J levels, as spacing between levels increases and relaxation slows down. Results of simulations are shown in Table 1. A slight but significant difference in parameter values, compared to that derived tentatively by others, was obtained. In order to further test the significance, we used the parameters derived by Tsuji et al. [9], and obtained worse fits for experimental and calculated spectra.

4. Conclusions

Ions formed by $(2+n; n \geq 1)$ resonance-enhanced-multiphoton-ionisation (REMPI) of acetylene, via gerade Rydberg states, were recorded as a function of laser power and frequency corresponding to the two-photon resonance excitation range $72\,500\text{--}83\,100\text{ cm}^{-1}$. The parent molecular ion, $C_2H_2^+$ was found to be the main product for the excitations to the $3p$ Rydberg states in the range $72\,500\text{--}75\,000\text{ cm}^{-1}$, while competition between parent ion and fragment ion formations was found for the $3p$ Rydberg states in the excitation region $75\,500\text{--}76\,200\text{ cm}^{-1}$. Fragment ion formations, on the other hand, were dominant in REMPI of the highest observed gerade Rydberg states between $82\,500$ and $83\,100\text{ cm}^{-1}$. Fragment ion signals for H^+ , C^+ and C_2^+ all showed analogous power dependence, different from that for the parent ion. Tracking potential energies for dissociation of various triplet and singlet energy-states of acetylene to C_2 and H_2 , via a *cis*-conformer using the STQN method for various basis sets and the B3LYP level of calculations, revealed energy minima for corresponding transition states in the energy region $75\,000\text{--}77\,000\text{ cm}^{-1}$. In light of the work of Hsu et al. [11], who identified a long-lived intermediate, most probably a *cis*-conformer, after two-photon excitation to the $3p^1\Sigma_g 0^0$ Rydberg state ($74\,279\text{ cm}^{-1}$), our observations suggest that the lowest energy transition state for the *cis*-conformer is a threshold for photodissociation of gerade Rydberg states to C_2 and H_2 . Hence, C_2^+ will be formed by additional three-photon ionisation of C_2 or by $(2+3)$ REMPI of C_2H_2 . Mechanisms are postulated involving $(2+3)$ REMPI of C_2H_2 to form C^+ as well as H^+ for resonance excitations larger than about $75\,000\text{ cm}^{-1}$.

REMPI spectra of partly-resolved rotational structured spectra corresponding to the transition $4p^1\Delta_g 0^0 \leftarrow X^1\Sigma_g^+$, recorded for

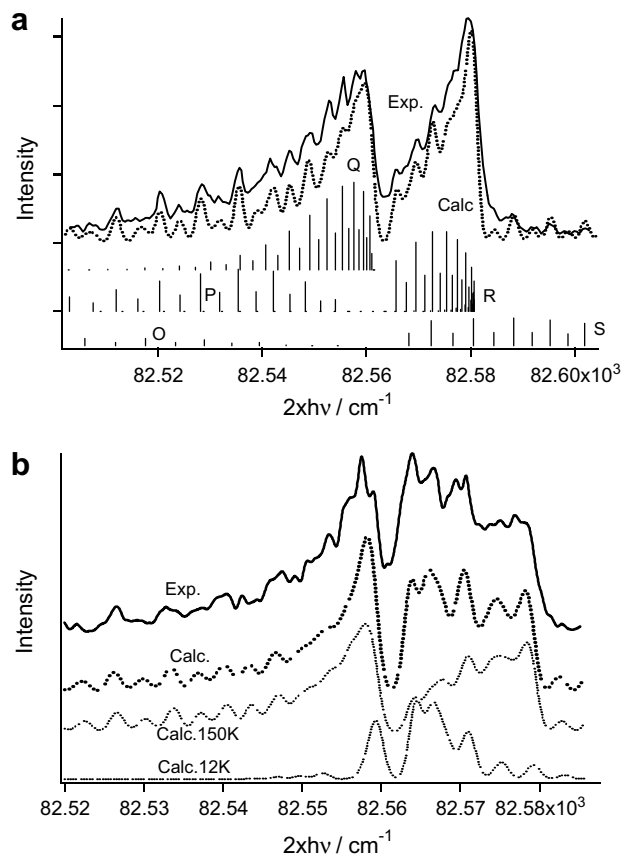


Fig. 4. Simulations of jet-cooled REMPI spectra due to the $4p^1\Delta_g 0^0 \leftarrow X^1\Sigma_g^+$ transition (a) Simulation of a REMPI spectrum; rotational temperature, $T = 220\text{ K}$. Top: experimental spectrum, middle: calculated spectrum, bottom: calculated rotational line contributions. (b) Simulation of a REMPI spectrum assuming two rotational temperature components (two Boltzmann rotational distribution components): (1) $T = 12\text{ K}$; (93%), (2) $T = 150\text{ K}$; (7%).

different jet cooling conditions, were simulated by a least square analysis procedure. A search was made for a unified solution, in terms of spectroscopic parameters and bandwidth, hence lifetime estimate. This method allowed determination of precise parameter values for the relevant excited Rydberg state.

Acknowledgements

The financial support of the University Research Fund, University of Iceland, and the Icelandic Science Foundation is gratefully acknowledged. We would also like to thank Dr. Andras Bodi for useful help with this project.

References

- [1] S. Boye et al., *J. Chem. Phys.* 116 (2002) 8843.
- [2] A. Campos, S. Boye, S. Douin, C. Fellows, J. Fillion, N. Shafizadeh, D. Gauyacq, *J. Phys. Chem.* 105 (2001) 9104.
- [3] N. Shafizadeh, J.H. Fillion, D. Gauyacq, S. Couris, *Philos. Trans. R. Soc. London, Ser. A-Math. Phys. Eng. Sci.* 355 (1997) 1637.
- [4] S. Boye, A. Campos, J. Fillion, S. Douin, N. Shafizadeh, D. Gauyacq, *C. R. Phys.* 5 (2004) 239.
- [5] S. Sorensen et al., *J. Chem. Phys.* 112 (2000) 8038.
- [6] A. Campos, S. Boye, P. Brechignac, S. Douin, C. Fellows, N. Shafizadeh, D. Gauyacq, *Chem. Phys. Lett.* 314 (1999) 91.
- [7] P. Löffler, E. Wrede, L. Schnieder, J. Halpern, W. Jackson, K. Welge, *J. Chem. Phys.* 109 (1998) 5231.
- [8] P. Löffler, D. Lacombe, A. Ross, E. Wrede, L. Schnieder, K. Welge, *Chem. Phys. Lett.* 252 (1996) 304.
- [9] K. Tsuji, N. Arakawa, A. Kawai, K. Shibuya, *J. Phys. Chem. A* 106 (2002) 747.
- [10] Y. Ganot, A. Golan, X. Sheng, S. Rosenwaks, I. Bar, *PCCP* 5 (2003) 5399.
- [11] Y. Hsu, M. Lin, C. Hsu, *J. Chem. Phys.* 94 (1991) 7832.
- [12] M. Ashfold, B. Tutcher, B. Yang, Z. Jin, S. Anderson, *J. Chem. Phys.* 87 (1987) 5105.
- [13] M.N.R. Ashfold, R.N. Dixon, J.D. Prince, B. Tutcher, *Mol. Phys.* 56 (1985) 1185.
- [14] M. Herman, R. Colin, *Phys. Scripta* 25 (1982) 275.
- [15] C. Peng, H.B. Schlegel, *Israeli J. Chem.* 33 (1994) 449.
- [16] C.Y. Peng, P.Y. Ayala, H.B. Schlegel, M.J. Frisch, *J. Comput. Chem.* 17 (1996) 49.
- [17] Á. Kvaran, H. Wang, *Mol. Phys.* 100 (2002) 3513–3519.
- [18] Á. Kvaran, K. Matthiasson, H. Wang, *Phys. Chem.; Indian J.* 1 (2006) 11.
- [19] Á. Kvaran, Ó.F. Sigurbjörnsson, H. Wang, *J. Mol. Struct.* 790 (2006) 27.
- [20] R.J. Donovan, R.V. Flood, K.P. Lawley, A.J. Yencha, T. Ridley, *Chem. Phys.* 164 (1992) 439.
- [21] D.S. Green, G.A. Bickel, S.C. Wallace, *J. Mol. Spectrosc.* 150 (1991) 388.
- [22] J.K.G. Watson, M. Herman, J.C.V. Crae, R. Colin, *J. Mol. Spectrosc.* 95 (1982) 101.
- [23] N. Govind, M. Petersen, G. Fitzgerald, D. King-Smith, J. Andzelm, *Comput. Mater. Sci.* 28 (2003) 250.
- [24] M.J. Frisch, et al., *GAUSSIAN 98*, Revision A.6. Gaussian, Inc., Pittsburgh PA, 1998.
- [25] K.M. Ervin et al., *J. Am. Chem. Soc.* 112 (1990) 5750.
- [26] Á. Kvaran, H. Wang, *J. Mol. Spectrosc.* 228 (2004) 143–151.
- [27] Á. Kvaran, H. Wang, B.G. Waage, *Can. J. Phys.* 79 (2001) 197.
- [28] Á. Kvaran, H. Wang, Á. Logadóttir, *J. Chem. Phys.* 112 (2000) 10811.
- [29] Á. Kvaran, Á. Logadóttir, H. Wang, *J. Chem. Phys.* 109 (1998) 5856.
- [30] R.G. Bray, R.M. Hochstrasser, *Mol. Phys.* 31 (1976) 1199.
- [31] Á. Kvaran, H. Wang, J. Ásgeirsson, *J. Mol. Spectrosc.* 163 (1994) 541.
- [32] K.F. Palmer, K.N. Rao, Mickelso Me, *J. Mol. Spectrosc.* 44 (1972) 131.
- [33] M.F. Jagod, M. Rosslein, C.M. Gabrys, B.D. Rehfuß, F. Scappini, M.W. Crofton, T. Oka, *J. Chem. Phys.* 97 (1992) 7111.